I J R B A T, Issue (X) Vol (II) May 2022: 112-120
A Double-Blind Peer Reviewed & Refereed Journal
OPEN ACCESS
e-ISSN 2347 – 517X
Original Article

INTERNATIONAL JOURNAL OF RESEARCHES IN BIOSCIENCES, AGRICULTURE AND TECHNOLOGY

 www.ijrbat.in

IMPACT OF CALCINATION ON OPTICAL PROPERTIES OF PRISTINE ZNO NANOPARTICLES SYNTHESIZED BY CHEMICAL PRECIPITATION

S. Sivakumar and Yengkokpam Robinson*
Department of Physics,
Annamalai University, Annamalai Nagar
Email: robinsonkokpam@gmail.com

Communicated : 08.03.2022 | Revision : 11.03.2022 Accepted :28.03.2022 | Published: 02.05.2022

ABSTRACT: In the context of science and technology, synthesis nanoparticles reveal new and innovative qualities that are supported by particular features such as size distribution, shape, and application of nano-sized materials. Zinc oxide is currently among the most prominent semiconductor oxides in nanomaterials. In this present work, a chemical precipitation method was used to study the structural, morphological, and optical properties of zinc oxide nanoparticles at room temperature. The obtained samples were characterized after different calcination at temperatures 500℃ and 700℃ by XRD, FTIR spectroscopy, SEM, EDAX, UV-DRS (UV-diffuse reflectance spectroscopy). XRD pattern analysis revealed that the samples exhibit a pure phase with a hexagonal wurtzite structure and their average crystallite sizes are in the nano-range of 23–30 nm. The formation of ZnO nanostructure was confirmed by FTIR analysis. SEM and EDAX exhibited the morphology and highly produced pure ZnO nanoparticles. The optical band gap energy of ZnO nanopowders was computed using UV-visible diffuse reflectance spectroscopy and was found to decrease from 3.31 eV to 3.19 eV. Due to its strong UV absorption, zinc oxide has a variety of beneficial applications, including sunscreen protectors and antiseptic ointments.

Key words: - zinc oxide, semiconductor, chemical precipitation method, band gap energy

INTRODUCTION :

Nanostructure metal oxide semiconductors with dimensions in the nanometer realm have attracted considerable interest in the fields of nanoscience, material science, biotechnology, information technology, and environmental technology as next-generation technologies [1]. Compared to their bulk materials, nanomaterials have distinct and significantly altered physical, chemical, and biological characteristics. Metal nanoparticles have attracted the interest of researchers due to their potential use in microelectronic devices, photocatalysis, magnetic devices, and powder metallurgy [2]. It has a large exciton binding energy of 60 meV and a direct wide band-gap of 3.37 eV with paramount n-type inorganic semiconductor material [3]. As particles get smaller in semiconductors, an extra influence known as the quantum size effect changes the band-gap size and hence the material's electrical characteristics. The radiative recombination efficiency of quantum dots built with indirect gap semiconductors has improved by several orders of magnitude [4]. The mineral zincite is found naturally in the earth's crust, although the vast majority of zinc oxide used in industry is synthesized. For this reason, particular emphasis has been placed on the development of nanoscale semiconducting materials [5]. ZnO nanoparticles are extremely important with prospective applications in optical, piezoelectric, magnetic, and gas sensing. It has been extensively employed because of its high catalytic efficiency, great adsorption ability, high isoelectric point electron, biocompatibility, electrical, optoelectronic, and photochemical characteristics [6,7]. ZnO appears hexagonal

wurtzite to be more stable than zinc blende and rock salt formations at room temperature. Based on structural and optical properties, defect and charge carrier control increase the performance of numerous ZnO applications. The chemical precipitation method was used in this study to synthesis ZnO samples, and their optical characteristics were examined at room temperature. This method yields nanoparticles of high purity and fine size by manipulating these parameters [8].

EXPERIMENTAL DETAIL:

Materials

Chemical precipitation is the finest technique for producing ZnO nanoparticles because it uses just two reaction reagents: a highly purified zinc precursor such as $Zn(NO_3)_2.6H_2O$ (zinc nitrate hexahydrate, 99%) and NaOH (sodium hydroxide, pellet min. 99%). All of the chemicals utilized in this method were analytical grade (AR) reagents purchased from Sigma-Aldrich Chemicals in India. De-ionized water was used as a dispersion solvent for the preparation and washing.

Synthesis of Pristine Zinc Oxide Nanoparticles

$Zn(NO_3)_2.6H_2O$ (zinc nitrate hexahydrate) and NaOH (sodium hydroxide) were used as precursors for the preparation of pristine ZnO nanoparticles using the chemical precipitation method. In the synthesis of pristine ZnO nanoparticles, 0.2 mol of zinc nitrate hexahydrate was first dissolved in 50 ml of de-ionized water in a beaker. A magnetic stirrer was used to fully dissolve the zinc nitrate hexahydrate at 700 rpm and 90℃. After the zinc nitrate hexahydrate had completely dissolved, 0.4 mol of sodium hydroxide was added to 50 ml of de-ionized water in a separate beaker. Under vigorous stirring, a molar ratio of 1:2 sodium hydroxide solution was steadily added dropwise, and the reaction mixture was stirred for 2 hours. The mixture solution produced gas during the reaction. A clear and homogeneous solution was formed once the reaction was completed. The obtained solution was cooled to room temperature before the supernatant liquid was carefully discarded. The acquired wet precipitate was filtered out, and the washing procedure was repeated several times with de-ionized water, ethanol, and acetone to remove organic/unwanted impurities and other unreacted substances from the obtained product. The white precipitates formed as a result of the reaction. The final product was given a break overnight before being heated in a hot air oven at 80℃ for 2 hours. Using an agate mortar, the dry precursor was crushed into a fine powder. Finally, the powdered products were calcined in a muffle furnace at different temperatures (500℃ and 700℃) for 2 hours and then stored in an airtight container for further analysis.

Instrumentation details

The x-ray diffractometer X'Pert Pro Powder model was used to analyze the crystal structure of the synthesized nanoparticles using Cu-Kα radiation (=1.5406Å) in the scan range with a step size of 0.017. The functional group was revealed by the Fourier Transform Infrared (FT-IR) spectra using a Perkin Elmer Spectrum Two model. The nature and particle size of ZnO nanoparticles were characterized using scanning electron microscopy (SEM) at room temperature on a JEOL – JSM 5610LV model. The composition of elements such as Zn and O was evaluated using energy-dispersive X-ray spectroscopy (EDAX). The sample was analyzed for optical band gap (E_g) energy at room temperature using a UV- DRS spectroscopy with model SHIMADZU-UV 2600. All experiments were carried out in triplicate, and the data collected was analyzed with the Origin Pro 2018 SR1 b9.5.1.195 software (Origin Lab Corporation, USA).

RESULTS AND DISCUSSION:

Structural Analysis

The structure and crystallinity of ZnO nanoparticles as-synthesis, 500℃ and 700℃ annealing temperatures were investigated using X-ray diffraction (XRD) at ambient temperature. In figure 1, the peaks observed in the XRD patterns of all the samples as-synthesis, 500℃, and 700℃ annealing temperatures were well matched when compared to JCPDS Card No. 89-0510, confirming that the synthesis products were pristine ZnO nanoparticles. In all of the samples, no distinctive peaks of impurity phases could be found. The peak intensity increases as the calcination temperature increases, attribute crystallinity, and validate the synthesized product's high purity [9]. Among these, the XRD pattern of ZnO 700℃ nanoparticles with more sharp peaks exhibited distinctive diffraction peaks corresponding to ZnO nanoparticles. The diffraction peaks identified at 2θ values of (31.77, 34.44, 36.28, 47.57, 56.57, 56.60, 62.87, 66.40, 67.11, 72.51 and 76.99) could be attributed to the hexagonal wurtzite structured diffraction plans (100), (002), (101), (102), (110), (103), (200), (112), (201), (004) and (202).

The crystalline size (D) of the samples were calculated using Debye Scherrer's formula from X-ray line broadening of the diffraction peaks:

$$D = \frac{k\lambda}{\beta \cos\theta}$$

where, D is the average crystallite size, k is the empirical constant equal to 0.9, λ is the wavelength of the x-ray radiation (λ = 1.5406 Å) (CuKα), θ is the Bragg diffraction angle and β is full width at half maximum (FWHM) of the respective diffraction peak.

Moreover, the structural parameters such as micro strain (ε), dislocation density (δ), lattice parameters (d) and unit cell volume (V) were also calculated from the XRD data using the formulae below [10,11]. The average crystallite size of the ZnO nanoparticles were in the nanometer range of 23 to 30 nm. The calculated values of crystallite size (D), microstrain (ε), dislocation density (δ), lattice parameters (d), and unit cell volume (V) are shown in Table 1.

FT-IR analysis

FTIR spectroscopy was used to assess the samples' composition, quality, and molecular structure. Figure 2 shows FTIR spectra observations of as-synthesis, ZnO 500°C, and ZnO 700°C annealing temperatures using the KBr technique at room temperature in the wavenumber range 400 cm^{-1} to 4000 cm^{-1}, with several peaks corresponding to the major absorption bands. The absorption peaks in the 700-400 cm^{-1} range could be assigned to the stretching modes of the Zn-O bond [12]. The broad absorption peaks ranging from 3550-3200 cm^{-1} indicated that the stretching vibration of the O-H stretching of the hydroxyl group was present in all samples. The absorption peaks in the 3000-2840 cm^{-1} range, which are attributed to the C-H stretching modes groups, indicate the existence of absorbed species on nanocrystals surfaces. The absorption peaks, which correspond to the C=C stretching mode of alkenes, are detected between 1670-1620 cm^{-1}. However, in the as-synthesis sample, an absorption peak at 1384 cm^{-1} was found, owing to the O-H bending of the hydroxyl group. The absorption peaks associated with C-N stretching were also detected in the 1250-1020 cm^{-1} region. The main absorption band's FTIR spectra are caused by Zn-O stretching at 445 cm^{-1}, 443cm^{-1}, 441 cm^{-1} for as-synthesis, ZnO 500°C, and ZnO 700°C annealing temperatures, respectively. These absorption bands are roughly equivalent to those reported in the literature [13-15].

MORPHOLOGICAL STUDIES:

The surface morphological and structural patterns of ZnO nanoparticles were studied using scanning electron microscopy (SEM). Figure 3 (a) and (c) show the SEM micrograph of the ZnO nanoparticles at different magnification

5K and 10K. The SEM analysis revealed ZnO nanoparticles with a homogeneous shape and size. As evident from SEM images, the particles are spherical and granular in form, with strongly agglomerated ZnO nanoparticles. The SEM picture of ZnO proves the existence of spherical nanoparticles with average diameters from 23 nm to 30 nm. The temperature change might lead to an increase in particle size. As a result, there is a close association between the SEM images and the XRD pattern [16,17].

Furthermore, SEM measurements confirmed that the synthesized ZnO nanoparticles were fine particles with crystalline morphology. It demonstrates that the ZnO nanoparticles are well distributed in powder form. Because of the attractive forces that exist between the ZnO nanoparticles, so every nanoparticle has considerable interaction with the surrounding nanoparticles with very few voids. The particle size of the suitably chosen optimal calcination temperature has a significant impact on the particle size of ZnO nanoparticles, and the particle size increases with a higher calcination temperature. The chemical synthesis and composition of the produced nanoparticles were investigated using the EDAX technique is shown in figure 3(c). The presence of the components zinc (Zn) and oxygen (O) in the nanoparticles was verified by EDAX spectra. As a result, the presence of pure ZnO nanoparticles after calcination in the sample with crystalline nature was achieved in the synthesis sample [18].

Fig. 3 (a) 5k, (b) 10k show the SEM micrograph of different magnification and 3 (c) shows the EDAX spectrum of pristine ZnO (700℃)

Optical Analysis

The optical absorption spectra were assessed using UV-visible diffuse reflectance spectroscopy (UV-DRS) at room temperature. Figure 4 depicts the optical absorption spectra of ZnO nanoparticles with various proportions as-synthesis, 500°C, and 700°C annealing temperatures. The absorption wavelength peaks in the UV range of around 200 and 400 nm are visible in all of the samples' spectra. The spectrum exhibits a distinctive absorption peak of ZnO at 370 nm, which may be attributed to intrinsic band-gap absorption and reflects the excitonic nature at ambient temperature. It was previously reported that the intrinsic band-gap absorption of ZnO nanoparticles is caused by electron transitions from the valence band to the conduction band (O2p Zn3d). In comparison to other calcinations, the absorbance maxima of the material calcined at 700°C are changed to higher wavelengths. Typically, the band-gap is calculated from absorbance spectra by considering the first derivative of the absorbance with respect to photon energy and seeking maxima on the lower energy sides of the derivative spectrum [19].

Fig. 4: UV-Vis absorption spectra (a) and band gap energy (b) of ZnO nanoparticles

The optical band gap energy values of pure ZnO nanoparticles were calculated using the standard Tauc's plot formula.

$$\alpha = \frac{\sqrt{A(h\nu - E_g)}}{h\nu}$$

where α is the absorption co-efficient, A is a constant value, $h\nu$ is the photon energy, and E_g is the energy band-gap. Using a graph, the band gap energy was computed by extrapolating a linear vertical curve to interpolate the energy axis. The optical band gap energy of the samples was found to vary from 3.31 eV to 3.19 eV, as indicated in table 1. A "blue shift" occurs when the Fermi level on the conduction band produces a broadening of the energy band [20]. The band gap of ZnO nanoparticles reduces when the calcination temperature is higher, an effect attributed to the increase in particle size of ZnO nanoparticles [21]. The product's strong UV absorption highlighted its applicability for medical uses such as sunscreen protectors and antiseptic ointments.

CONCLUSION:

The findings of the study showed that the properties of zinc oxide nanoparticles prepared using the chemical precipitation approach were improved. The XRD pattern indicated that the produced samples have a hexagonal wurtzite structure with an average crystallite size ranging from 23 nm to 30 nm. The shape and excellent purity of ZnO nanoparticles were shown by SEM and EDAX. The band gap energy was found to decrease from 3.31 eV to 3.19 eV while calcination increased. Zinc oxide possesses advantageous applications such as sunscreen protectors and antiseptic ointments.

ACKNOWLEDGMENTS:

Author Yengkokpam Robinson is thankful to the Prof. and Head, Department of Physics, Annamalai University, for providing the necessary laboratory facilities to carry out this work and received financial support from the Ministry of Electronics and Information Technology, India through North Eastern Council (MN202021010699339).

Declaration of competing interest

On behalf of all authors, the corresponding author states that there is no conflict of interest regarding to this work.

REFERENCES:

Sangeetha, G., Rajeshwari, S., & Venckatesh, R. (2011). Green synthesis of zinc oxide nanoparticles by aloe barbadensis miller leaf extract: Structure and optical properties. Materials Research Bulletin, 46(12), 2560-2566. https://doi.org/10.1016/j.materresbull.2011.07.046

Yadav, A., Prasad, V., Kathe, A. A., Raj, S., Yadav, D., Sundaramoorthy, C., & Vigneshwaran, N. (2006). Functional finishing in cotton fabrics using zinc oxide nanoparticles. Bulletin of materials Science, 29(6), 641-645. https://doi.org/10.1007/s12034-006-0017-y

Hasanpoor, M., Aliofkhazraei, M., & Delavari, H. (2015). Microwave-assisted synthesis of zinc oxide nanoparticles. Procedia Materials Science, 11, 320-325. https://doi.org/10.1016/j.mspro.2015.11.101

Rajalakshmi, M., Arora, A. K., Bendre, B. S., & Mahamuni, S. (2000). Optical phonon confinement in zinc oxide nanoparticles. Journal of Applied Physics, 87(5), 2445-2448. https://doi.org/10.1063/1.372199

Mirzaei, H., & Darroudi, M. (2017). Zinc oxide nanoparticles: Biological synthesis and biomedical applications. Ceramics International, 43(1), 907-914. https://doi.org/10.1016/j.ceramint.2016.10.051

Hao, Y. M., Lou, S. Y., Zhou, S. M., Yuan, R. J., Zhu, G. Y., & Li, N. (2012). Structural, optical, and magnetic studies of manganese-doped zinc oxide hierarchical microspheres by self-assembly of nanoparticles. Nanoscale Research Letters, 7(1), 1-9. https://doi.org/10.1186/1556-276X-7-100

Tan, T. L., Lai, C. W., & Abd Hamid, S. B. (2014). Tunable band gap energy of Mn-doped ZnO nanoparticles using the coprecipitation technique. Journal of Nanomaterials, 2014. https://doi.org/10.1155/2014/371720

Thambidurai, S., Gowthaman, P., Venkatachalam, M., Suresh, S., & Kandasamy, M. (2021). Morphology dependent photovoltaic performance of zinc oxide-cobalt oxide nanoparticle/nanorod composites synthesized by simple chemical co-precipitation method. Journal of Alloys and Compounds, 852, 156997. https://doi.org/10.1016/j.jallcom.2020.156997

Thambidurai, S., Gowthaman, P., Venkatachalam, M., & Suresh, S.

(2020). Enhanced bactericidal performance of nickel oxide-zinc oxide nanocomposites synthesized by facile chemical co-precipitation method. Journal of Alloys and Compounds, 830, 154642. https://doi.org/10.1016/j.jallcom.2020.154642

Sundaram, P. S., Sangeetha, T., Rajakarthihan, S., Vijayalaksmi, R., Elangovan, A., & Arivazhagan, G. (2020). XRD structural studies on cobalt doped zinc oxide nanoparticles synthesized by coprecipitation method: Williamson-Hall and size-strain plot approaches. Physica B: Condensed Matter, 595, 412342. https://doi.org/10.1016/j.physb.2020.412342

Mukhtar, M., Munisa, L., & Saleh, R. (2012). Co-precipitation synthesis and characterization of nanocrystalline zinc oxide particles doped with Cu 2+ ions. http://dx.doi.org/10.4236/msa.2012.38077

Sharma, N., Jandaik, S., Kumar, S., Chitkara, M., & Sandhu, I. S. (2016). Synthesis, characterisation and antimicrobial activity of manganese-and iron-doped zinc oxide nanoparticles. Journal of Experimental Nanoscience, 11(1), 54-71. https://doi.org/10.1080/17458080.2015.1025302

Okpara, E. C., Fayemi, O. E., Sherif, E. S. M., Junaedi, H., & Ebenso, E. E. (2020). Green wastes mediated zinc oxide nanoparticles: synthesis, characterization and electrochemical studies. Materials, 13(19), 4241. https://doi.org/10.3390/ma13194241

Udhayan, S., Udayakumar, R., sagayaraj, R., & Gurusamy, K. (2021). Evaluation of Bioactive Potential of a Tragia involucrata Healthy Leaf Extract @ ZnO Nanoparticles. Journal of Bionanoscience, 1-17. https://doi.org/10.1007/S12668-021-00864-Z

Dole, B. N., Mote, V. D., Huse, V. R., Purushotham, Y., Lande, M. K., Jadhav, K. M., & Shah, S. S. (2011). Structural studies of Mn doped ZnO nanoparticles. Current Applied Physics, 11(3), 762-766. https://doi.org/10.1016/j.cap.2010.11.050

Singh, R. P., Shukla, V. K., Yadav, R. S., Sharma, P. K., Singh, P. K., & Pandey, A. C. (2011). Biological approach of zinc oxide nanoparticles formation and its characterization. Adv. Mater. Lett, 2(4), 313-317. http://dx.doi.org/10.5185/amlett.indias.204

Zak, A. K., Razali, R., Abd Majid, W. H., & Darroudi, M. (2011). Synthesis and characterization of a narrow size distribution of zinc oxide nanoparticles. International journal of nanomedicine, 6, 1399. http://dx.doi.org/10.2147/IJN.S19693

Khan, S. A., Shahid, S., Bashir, W., Kanwal, S., & Iqbal, A. (2017). Synthesis, characterization and evaluation of biological activities of manganese-doped zinc oxide nanoparticles. Tropical Journal of Pharmaceutical Research, 16(10), 2331-2339. https://doi.org/10.4314/tjpr.v16i10.4

Arya, S., Lehana, P. K., & Rana, S. B. (2017). Synthesis of zinc oxide nanoparticles and their morphological, optical, and electrical characterizations. Journal of Electronic Materials, 46(7), 4604-4611. https://doi.org/10.1007/s11664-017-5469-x

Kaur, M., Kaur, P., Kaur, G., Dev, K., Negi, P., & Sharma, R. (2018). Structural, morphological and optical properties of Eu-N co-doped zinc oxide nanoparticles

synthesized using co-precipitation technique. Vacuum, 155, 689-695. https://doi.org/10.1016/j.vacuum.2018.06.046

Kumar, S. S., Venkateswarlu, P., Rao, V. R., & Rao, G. N. (2013). Synthesis, characterization and optical properties of zinc oxide nanoparticles. International Nano Letters, 3(1), 1-6. https://doi.org/10.1186/2228-5326-3-30

Table 1. Comparison the structural size of ZnO nanoparticles

Materials	*Crystallite size (nm)*	*Dislocation density (δ)* x 10^{15}[m^{-2}]	*Micro-strain (ε)* x 10^{-3}	*Lattice parameters*		*Unit cell volume (V)* ($Å^3$)	*Band gap energy(E_g)* (eV)
				a (Å)	c (Å)		
ZnO(as-synthesis	23.03	1.8854	1.6438	3.255	5.2126	47.89	3.31
ZnO(500℃)	25.87	1.4938	1.4015	3.251	5.2105	47.69	3.27
ZnO(700℃)	29.81	1.1252	1.2438	3.252	5.2110	47.73	3.19

Fig. 1: X-ray diffraction patterns of ZnO nanoparticles

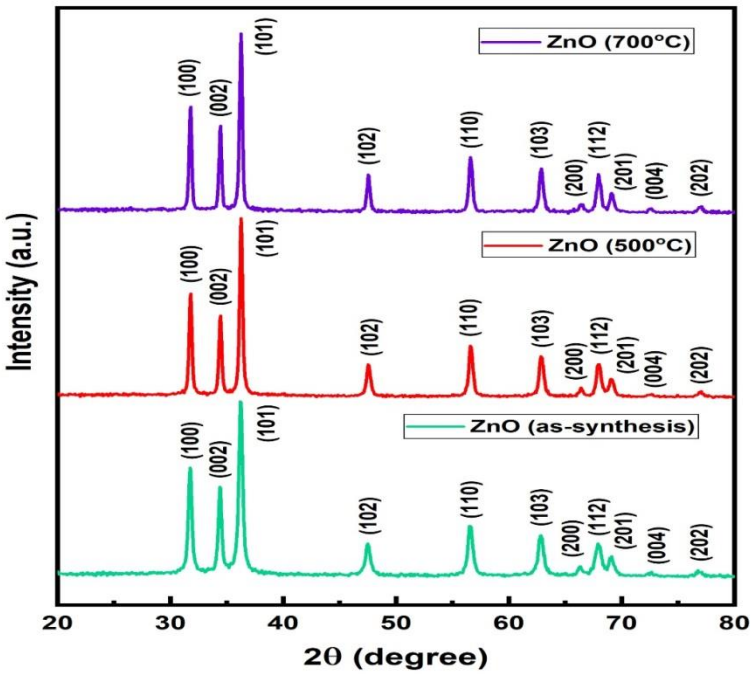

Fig. 2: FTIR spectra of ZnO (as-synthesis, 500℃, 700℃) nanoparticles

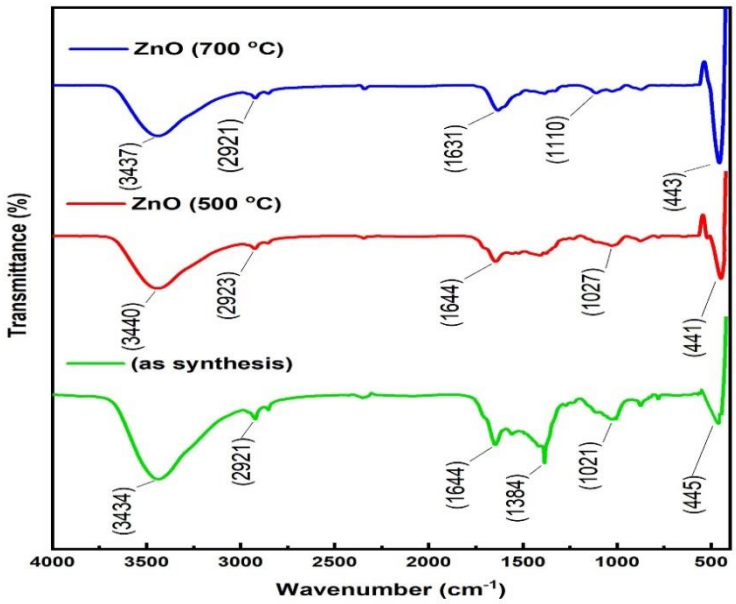

Fig. 3 (a) 5k, (b) 10k show the SEM micrograph of different magnification and 3 (c) shows the EDAX spectrum of pristine ZnO (700℃)

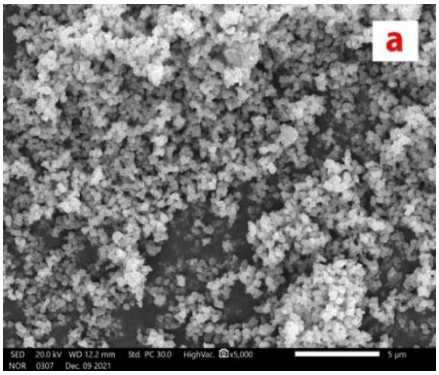

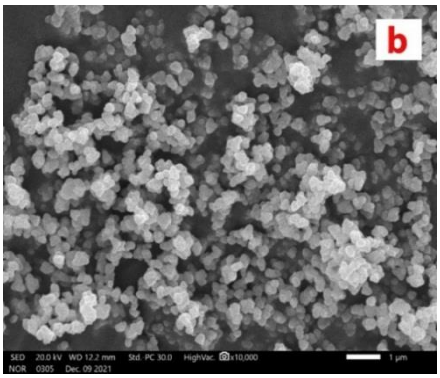

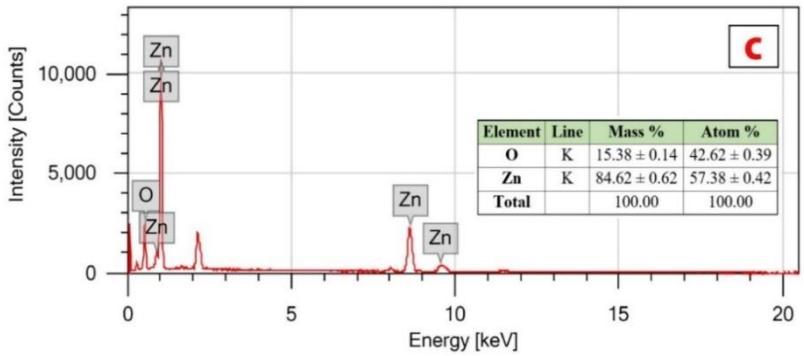

Fig. 4: UV-Vis absorption spectra (a) and band gap energy (b) of ZnO nanoparticles